Optica Applicata, Vol. XXI, No. 4, 1991

High precision reflectometer for surface layer characterization *

K. Jezierski, Z. Gumienny, J. Misiewicz

Institute of Physics, Technical University of Wrocław, Wybrzeże Wyspiańskiego 27, 50–370 Wrocław, Poland.

A new high-precision reflectometer has been constructed for energy range 2–6 eV. Normal incidence of light beam and computer control are applied. The exemplary results of measurements are discussed. Surface microroughness for surfaces prepared in different ways is estimated. The experimental data are compared with the results obtained for the surfaces simulated by means of fractal model. The structure of surface layer for implanted GaAs is discussed taking into account EMA theory and multilayer model. The results of ellipsometric spectroscopy are compared with those obtained by Kramers–Kronig analysis of reflectance spectrum, using additionally the ellipsometric data for one energy point.

1. Introduction

Optical measurements based on reflectometry are widely used for characterization of different materials, due to their simplicity and nondestructive character. One of the simplest methods is the measurement of the reflectance spectrum, i.e., the ratio of the reflected to the incident light intensity in a given energy range [1], [2]. In many cases, the results of reflectance measurements have been interpreted in terms of the structure of the optical constants spectra for bulk material (see, for example, [3]–[5]). Although the influence of surface artifacts has been pointed out many times [6]–[9], it was regarded as the experimental error rather than a valuable source of information about the surface layer. This fact was connected with difficulties in obtaining very high accuracy of the reflectance spectra measurements. The other methods, like ellipsometric measurements [10], total integrated scattering measurements [11], or photoreflective spectroscopy [12], were regarded as a more promising tool for analysing the surface layer.

We have taken efforts to construct a very precise reflectometer in order to get results comparable with the ones obtained by other optical methods that are quite often more expensive and more laborious. The experimental set-up is presented in Sect. 2. The idea of normal incidence was taken advantage of, and a special optical set-up for sample alignment as well as microcomputer control were applied. The

---

* This work was partially sponsored by the Ministry of National Education by a grant DNS-P/04/190/90-2, 31275-6.

measurements were carried out in the visible and ultraviolet ranges to provide sensitivity to the surface microroughness (see Sect. 3). When required, the analysis of the surface layer can be more advanced than in the presence of microroughness. In Section 4, the results obtained for the implanted GaAs samples are presented. The multilayer model was applied and the profile of the degree of amorphousness was determined. In Section 5, the results of spectroscopic ellipsometry and the results of Kramers–Kronig analysis of reflectance spectra are compared.

2. Experiment

The experimental set-up (see Fig. 1) was designed for the measurements of the reflectance for a given sample in relation to the reflectance for the reference sample within the energy range from 2 to 6 eV. The normal incidence of the light beam as well as microcomputer control were applied.

The deuter lamp was used as the light source for the double prism monochromator KB5601 (COBRABID). The xenon lamp can also be mounted for initial aligning of the system and for measurements in the limited energy range. Behind the monochromator the beam is modulated with constant frequency $f = 500$ Hz (see Fig. 2). Also the exchangeable field diaphragm D_f is used for creating the light spot on the sample (with diameters from 0.3 to 2.0 mm). The optical set-up consisting of five quartz lenses and a special cube for light beam division images the light spot on both samples: the one being measured and the reference one. The reflected signal is chosen by the system of two blinds controlled by the microcomputer. The lock-in and photomultiplier (M12FQ51) are applied to detect the intensity of light beam. The signal from the lock-in is the input signal for the microcomputer after A/D conversion. The microcomputer controls also the step-motor for the wavelength changes in the monochromator.

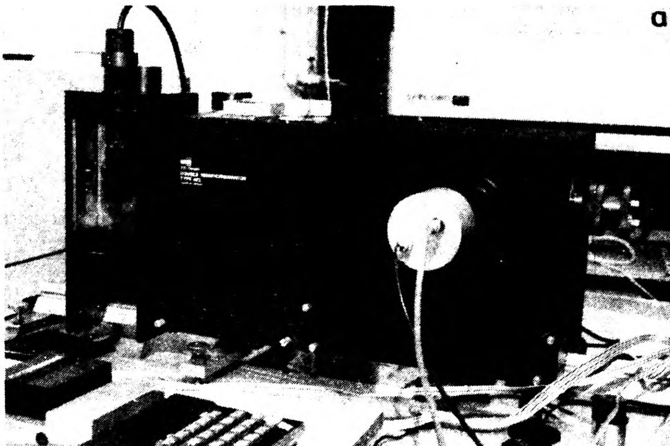

Fig. 1a

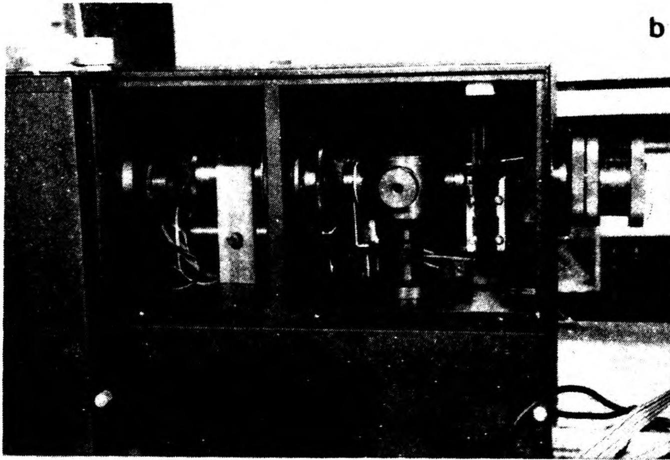

Fig. 1. Photographs of the experimental set-up: during work (a), and inside the chamber (b)

Special attention is directed towards the sample holders with four degrees of freedom and the aligning process after mounting each sample in the set-up. During aligning the eypiece is mounted instead of the photomultiplier. In the visible range, the light beam can be easily focused on the sample surfaces and the interference image can be observed. Therefore, the samples can be parallel with the accuracy of $\lambda/4$ in the region of the light spot on the sample.

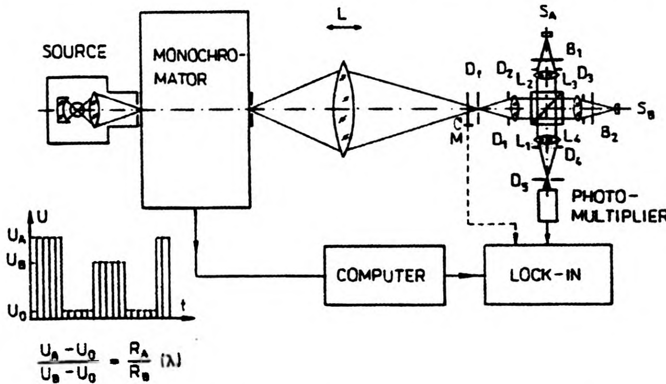

Fig. 2. Schematic diagram of the experimental set-up for reflectance measurements: L — quartz lenses, D — diaphragms, M — modulator, B — automatic blinds, S — samples. In the insert, the detected signal vs time is presented (R_A and R_B are the reflectances for the samples A and B, respectively)

The measurement is carried out in a given energy range with a given accuracy point by point. In each point, the signals from the samples are detected many times and then the averaging procedure is carried out. The background signal can be also taken into account (see insert in Fig. 2). The averaging procedure consists of two steps. The first gives us the value of the signal with the approximately constant absolute error. It is carried out for R_A and for R_B and the value of R_A/R_B can be

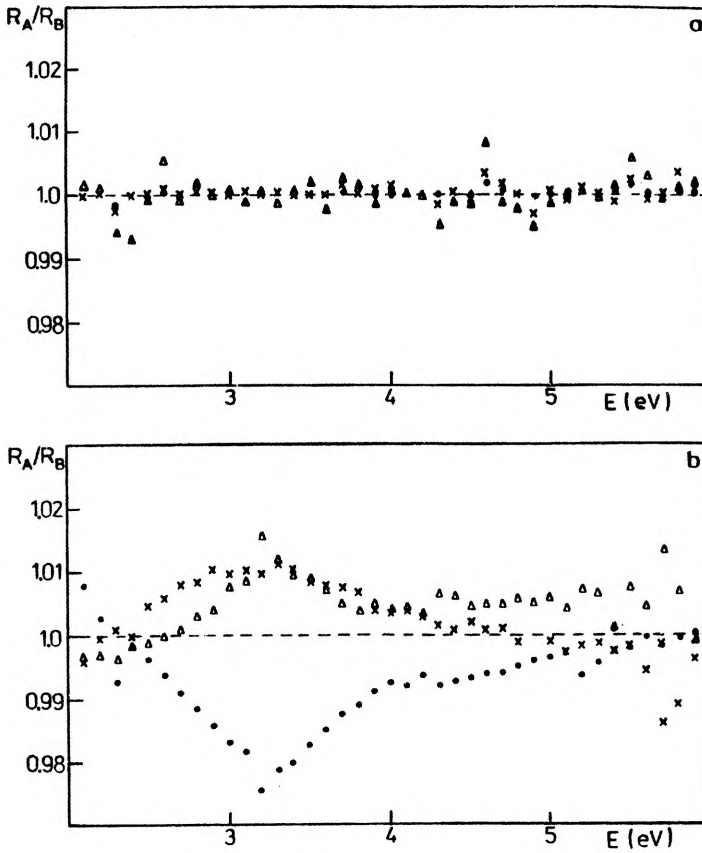

Fig. 3. Test results for Al thin film: a — the mean values of R_A/R_B after one (△), three (×), and five (●) simple measurements for the same aligning; b — the three different R_A/R_B spectra (△, ×, ●), when the aligning was repeated for each spectrum measurement. In all cases the lack of an error means $R_A/R_B=1$, because R_A and R_B are the reflectances for the same sample

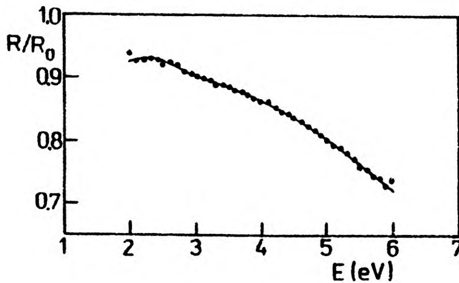

Fig. 4. Exemplary reflectance data obtained for Al surfaces prepared in different ways

calculated. Then, in the second step, this procedure is repeated several times and the mean value of R_A/R_B is determined. The measuring subroutine is complicated because of the use of one photomultiplier in the experiment, and thus the simple rule — the longer the measurement of the signal, the higher the accuracies — cannot be

applied. It is known that in such an experiment, the error connected with the aligning process will appear. So, it is recommended to repeat the aligning procedure and the whole spectrum measurements several times. In Figure 3, we can see the test results obtained for aluminium thin films. For an ideal measurement, in this case we should obtain in the whole energy range $R_A/R_B = 1$. In Figure 3a, we can see the results when the second step of the averaging procedure is repeated 1, 3 and 5 times. The error is almost constant in the whole energy range. However, one can see in Fig. 3b that the dominant part of the final error is due to uncertainty of the aligning process. Taking into account the test results, the accuracy of our measurement can be estimated to be $\Delta R = 0.005$ for the individual spectrum measurement and $\Delta R = 0.02$ when the whole aligning process is considered.

The exemplary results of the measurements for the aluminium thin films are shown in Fig. 4. The reflectance R for the Al film after ion etching process was determined in relation to the reflectance R_0 for the Al film before this process. The obtained spectrum R/R_0 can be discussed taking into account the influence of the surface microroughness (see Sect. 3).

In our case, the measured reflectance is always given in relation to the reflectance of the reference sample. This fact can be regarded as an additional source of the experimental error because of the lack of the ideal reference samples. However, our set-up is designed specially for investigation of the changes in reflectance spectra, for example, the changes due to the sample surface preparation process. In such cases the ideal reference sample is not necessary because the numerical analysis is based only on the relative R/R_0 spectrum or the R_0 values can be taken from another measurement without destroying the results.

3. Determination of the surface microroughness

Reflectance is very sensitive to the surface roughness [6]–[8], [13], [14]. The reflected light changes drastically its intensity due to the roughnesses in scale or larger than wavelength. Therefore, the infrared region is very sensitive to the macroroughness (waviness of the surface), whereas visible and ultraviolet regions to the microroughness. When we want to determine the influence of the surface roughness on the reflectance, the following formula is often used:

$$R/R_0 = \exp\left(-\frac{16\pi^2}{h^2c^2}E^2\sigma^2\right) + R_{non}(\sigma, \beta, T, E) \tag{1}$$

where R_0 is the reflectance for the flat surface. The first term in formula (1) is connected with the specular reflection, and the second with the nonspecular one; σ is the rms roughness, T is the correlation length, and the parameter β denotes the acceptance angle in a given measurement set-up. The explicit form of the nonspecular term depends on the model of surface roughness applied [13], [15]. We can predict two very different experimental situations: the first when the first term in formula (1) dominates and the $\ln(R/R_0)$ vs E^2 plot is linear, and the second when the nonspecular term in formula (1) dominates. These situations are illustrated in Fig. 5

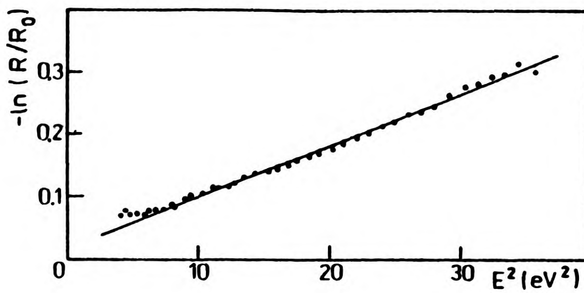

Fig. 5. Reflectance data taken from Fig. 4 presented in $-\ln(R/R_0)$ vs E^2 scale (slope of the line gives us the value of $\sigma = 8.8$ nm)

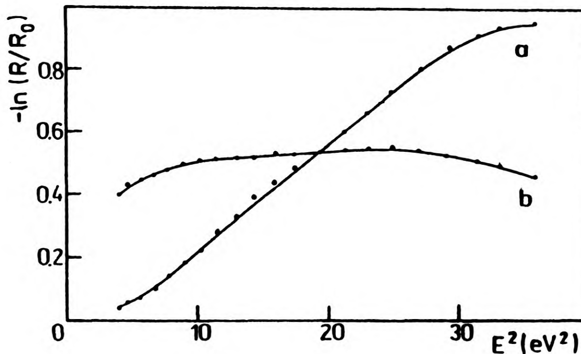

Fig. 6. Reflectance spectra for GaAs surfaces polished in different ways (for curve a the value of $\sigma = 18.4$ nm)

and Fig. 6 by the experimental data. When the first situation takes place, the value of rms roughness σ can be given from the experiment with great precision. In our case, the error $\Delta\sigma$ is equal to 0.5 nm, but the minimal difference in σ between the measured surfaces should be about 3 nm due to the test results shown in Fig. 3.

In order to discuss the experimental R/R_0 curves when the diffuse reflection is noticeable a model for the surface roughness should be applied. In this paper, the results for fractal model of surface roughness generation are presented. The generation algorithm was decribed in detail elsewhere [16], [17]. In Figure 7, we can see the profiles for surfaces obtained for the different values of generation parameters. The values of the parameter r (connected with the roughness height, see formula (2) in [17]) were equal to 1 μm (Fig. 7a), 250 nm (Fig. 7b), and 100 nm (Fig. 7c). For the generated surfaces, the R/R_0 spectra in the energy range 2–6 eV were calculated by means of the classical Fresnel–Kirchhoff diffraction formula. The results are shown in Fig. 8. For the flattest surface, we can see the straight line (curve c) which means that only the specular reflection is present, and for the roughest surface (curve a) one can see domination of the nonspecular term.

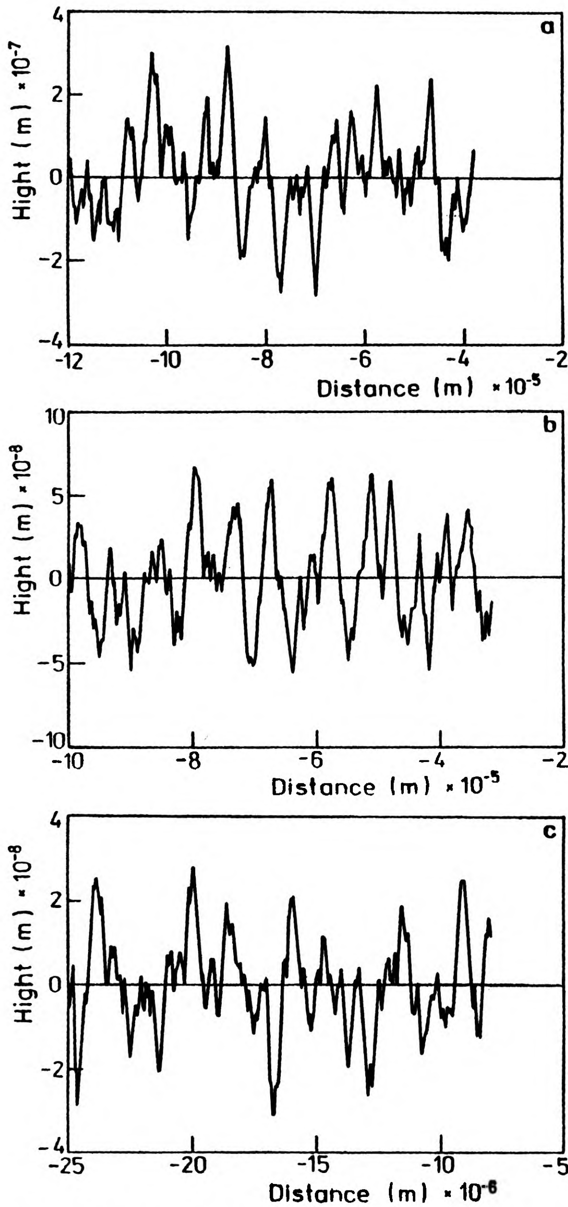

Fig. 7. Profiles for the surfaces generated by means of fractal model obtained for the different values of parameter r: 1 μm (**a**), 250 nm (**b**), and 100 nm (**c**)

4. Analysis of the disturbed surface layer

When the reflectance is measured for the sample with disturbed surface layer, a careful computer analysis of the spectrum gives us information about structure of the surface layer. Let us present the exemplary results of such analysis obtained for the implanted GaAs samples [18], [19].

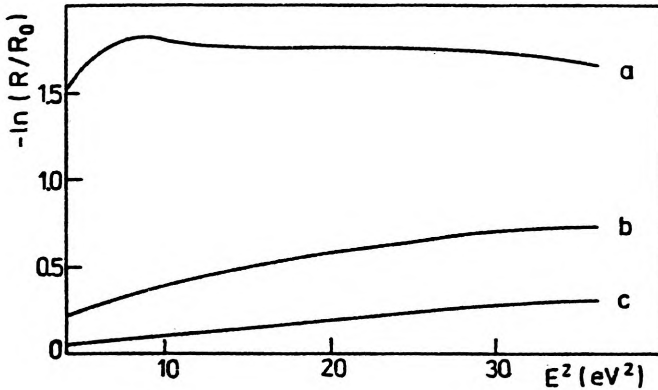

Fig. 8. Reflectance spectra for the surfaces presented in Fig. 7. For the curve c the value of $\sigma = 8.8$ nm can be determined

The ion implantation process is the source of defects in the surface layer. The concentration of ions and defects in the implanted layer are not homogeneous but are a function of the distance from the surface of the sample. Therefore, the surface layer is regarded as a multilayer consisting of the thin parallel-sided lamellae. Each lamella is described by the degree of amorphousness q because it is a mixture of the crystalline and amorphous phases, according to our assumption. This assumption and the EMA theory yield the following formula for the dielectric permittivity $\tilde{\varepsilon}$:

$$q\frac{\tilde{\varepsilon}_a-\tilde{\varepsilon}}{\tilde{\varepsilon}_a+2\tilde{\varepsilon}}+(1-q)\frac{\tilde{\varepsilon}_c-\tilde{\varepsilon}}{\tilde{\varepsilon}_c+2\tilde{\varepsilon}}=0 \tag{2}$$

where $\tilde{\varepsilon}_a$ and $\tilde{\varepsilon}_c$ are the complex permittivities of amorphous phase and crystalline phase, respectively. The reflectance for the parallel uniform layers system was calculated by means of characteristic matrices approximation [20]. A comparison between the calculated reflectance spectrum and the measured one enables us to determine the profile of the degree of amorphousness.

We present below the exemplary results of such a procedure applied to the GaAs n-type crystals implanted with the Al^+ ions. The energy of ions was 100 keV and the doses were from 10^{13} to 10^{15} cm^{-2}. The R/R_0 (R_0 — reflectance for the unimplanted sample) spectra are shown in Fig. 9a. Using the simple fitting procedure for each surface the profile of q was calculated (see Fig. 9b). The assumption about the Gaussian shape of the profile was made

$$q(x) = q_0\exp[(x-x_{max})^2/2s^2] \tag{3}$$

where x_{max} is the parameter independent of the dose and equal to 60 nm due to the results of PIPE measurements [19]. The values of q_0 and s were chosen to obtain the best fit for the reflectance data. The additional relation $q(x) = 1$ was applied, with $q(x)$ from relation (3) being greater than 1.

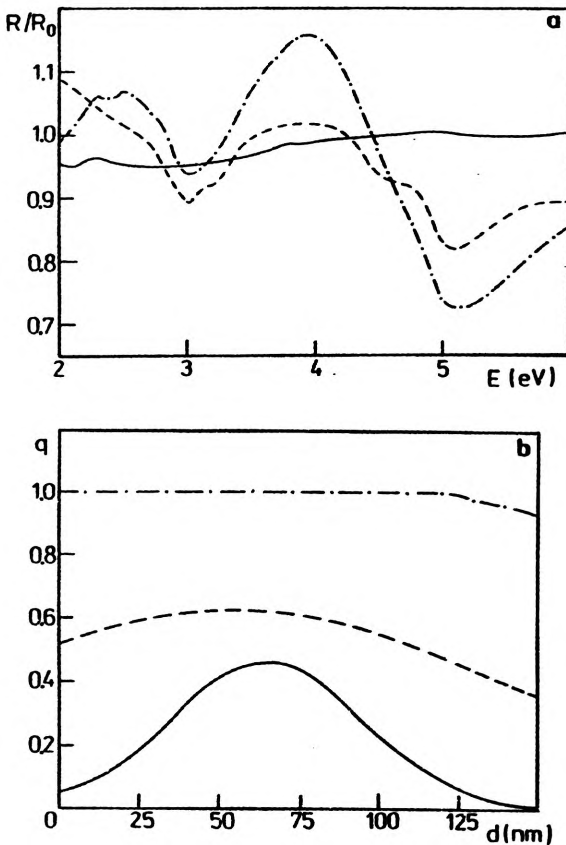

Fig. 9. Reflectance spectra measured for the implanted GaAs, R, in relation to the unimplanted GaAs sample, R_0, (a) and the determined profiles of the degree of amorphousness for the implanted samples (b). The implantation process was made with Al^+ ions of the energy 100 keV and with the doses (in cm^{-2}): 10^{13} (solid line), 10^{14} (dashed line), and 10^{15} (dotted-dashed line)

5. Kramers–Kronig analysis of the reflectance data

The reflectance data are not only the subject of the straightforward treatment, as described in the previous section, but they are also the initial data for the determination of the optical constants spectra (e.g., the complex refractive index $\tilde{n} = n + ik$) [21], [22]. According to the well-known Kramers-Kronig relation

$$\theta(E_0) = \frac{E_0}{\pi} \int_0^\infty \frac{\ln R(E)}{E_0^2 - E^2} dE \tag{4}$$

the phase shift θ of the electromagnetic wave on reflection can be calculated. Then the refractive index n and the extinction coefficient k are determined:

$$n = \frac{1-R}{1+R-2\sqrt{R}\cos\theta}, \tag{5}$$

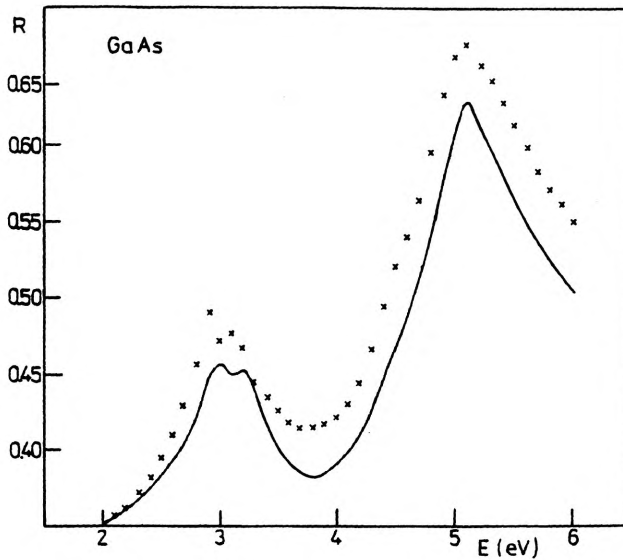

Fig. 10. Reflectance spectrum measured for high quality GaAs surface (solid line) and the results taken from the spectroscopic ellipsometry measurement [21] (crosses)

$$k = \frac{2\sqrt{R}\cos\theta}{1+R-2\sqrt{R}\cos\theta}. \tag{6}$$

In our case, the reflectance data in the energy range from 2 eV to 6 eV are given. The integral (4) requires the reflectance spectrum also below 2 eV and over 6 eV. It can be provided by means of the extrapolation procedures taking into account the additional data [23], [24].

In Figure 10, the reflectance spectra for GaAs are shown. We would like to show the accuracy of Kramers–Kronig analysis by comparing its results with the results of spectroscopic ellipsometry. Therefore, the calculations were based on the reflectance data given by ASPNES and STUDNA [25]. Additionally, we assumed that below the energy gap ($E \leqslant 1.425$ eV) the absorption coefficient is equal to zero and that the optical constants are known for 1.959 eV (due to the widely used ellipsometers based on the He-Ne laser with the 632.8 nm line). The last assumption means that our set of the experimental data consists of two items for each sample: the reflectance spectrum in the energy range 2–6 eV and the ellipsometric measurements results for one energy point – 1.959 eV. The use of the extrapolation procedures described in [23], [24] gives us the results shown in Fig. 11. The extrapolations cannot be determined explicitly and the extrapolation error appears. Therefore, in Fig. 10, the optical spectra determined are shown together with the estimation of the extrapolation error range. The agreement obtained between the Kramers–Kronig analysis results and spectroscopic ellipsometry ones seems to be satisfactory. There is no difference in the structure of the spectra. Though the values of n and k are given with the absolute error 0.2, for many energy points the error reaching 0.05 is distinctly smaller.

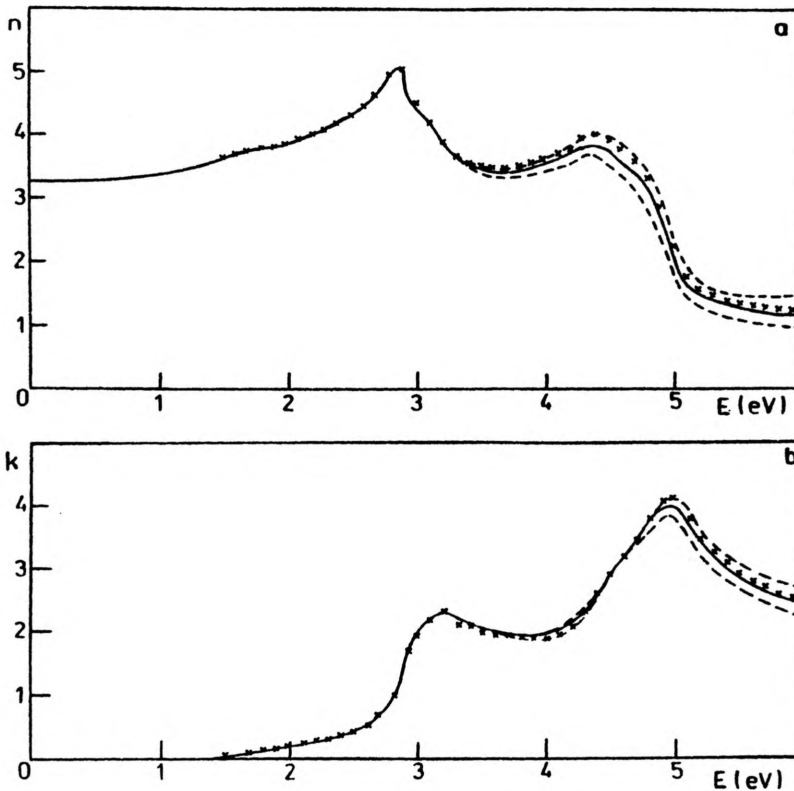

Fig. 11. Optical constants spectra for GaAs calculated by means of Kramers–Kronig analysis (solid line), the estimation of extrapolation error (dashed lines), and the results taken from the spectroscopic ellipsometry measurement [21] (crosses): a – spectra of the refractive index, b – spectra of the extinction coefficient

6. Conclusions

Analysis of the experimental data obtained by means of the new reflectometer gives satisfactory results. There is a good agreement with the results of other optical techniques. In the case of implanted layer analysis, the agreement with the results of ellipsometric measurements [18] can be noticed and in the case of Kramers–Kronig analysis test the comparison is made with the spectroscopic ellipsometry. Certainly, when the most accurate results are required, the most sophisticated optical methods should be applied. But in many cases the reflectance spectrum measurement and the computer analysis of the data seem to be adequate.

The experimental set-up enables us to perform measurements in polarized light. A very interesting feature is connected with the normal incidence of the light beam. For example, the sample may be placed in quartz cuvette with etching solution.

We would also like to emphasize the importance of the computer analysis of the experimental data. Some additional assumptions enable us to draw explicit con clusions in the majority of cases.

References

[1] KISIEL A., PODÓRNY M., RODZIK A., TUROWSKI M., Opt. Appl. **9** (1979), 249.
[2] OLESZKIEWICZ J., PODGÓRNY M., KNAPIK J., KISIEL A., Opt. Appl. **15** (1985), 163.
[3] HARBEKE G., Phys. Status Solidi **27** (1968), 9.
[4] GRASSO V., PERILLO P., Solid State Commun. **21** (1977), 323.
[5] LEVEQUE G., BERTRAND Y., ROBIN J., J. Phys. C: Solid State Phys. **10** (1977), 343.
[6] BENNET H. E., J. Opt. Soc. Am. **53** (1963), 1389.
[7] BENNET H. E., PORTEUS J. O., J. Opt. Soc. Am. **51** (1961), 123.
[8] KARNICKA-MOŚCICKA K., KISIEL A., Surf. Sci. **121** (1982), L545.
[9] MORRISON R., F., Phys. Rev. **124** (1961), 1314.
[10] AZZAM R. M. A., BASHARA N. N., *Ellipsometry and Polarized Light*, North-Holland, Amsterdam 1977.
[11] ROCHE P., PELLETIER E., Appl. Opt. **23** (1984), 3561.
[12] MISIEWICZ J., ZHENG X., BECLA P., HEIMAN D., Solid State Commun. **66** (1988), 351.
[13] PORTEUS J. O., J. Opt. Soc. Am. **53** (1963), 1394.
[14] FILIŃSKI I., Phys. Status Solidi B **49** (1972), 577.
[15] BECKMANN P., SPIZZICHINO A., *The Scattering of Electromagnetic Waves from Rough Surfaces*, Pergamon, Mcmilian, London, New York 1963.
[16] ŁĄTKA M., JEZIERSKI K., Opt. Appl. **19** (1989), 113.
[17] JEZIERSKI K., ŁĄTKA M., *Proc. 4th Conf. on Surface Physics*, Łódź 1989, p. 206.
[18] KULIK M., JEZIERSKI K., Acta Phys. Pol. Ser. A **75** (1989), 211.
[19] JEZIERSKI K., KULIK M., Opt. Commun. **71** (1989), 285.
[20] PALIK E. D., *Handbook of Optical Constants of Solids*, Academic Press, London 1985.
[21] STERN F., Solid State Phys. **15** (1963), 299.
[22] JEZIERSKI K., MISIEWICZ J., WNUK J., PAWLIKOWSKI J. M., Opt. Appl. **11** (1981), 571.
[23] JEZIERSKI K., J. Phys. C: Solid State Phys. **17** (1984), 475.
[24] JEZIERSKI K., J. Phys. C: Solid State Phys. **19** (1986), 2103.
[25] ASPNES D. E., STUDNA A. A., Phys. Rev. B **27** (1983), 985.

Received May 10, 1991,
in revised form November 18, 1991